MATERIALS CHEMISTRY FRONTIERS

CCS 中国化学会 CHINESE CHEMICAL SOCIETY

ICCAS

ROYAL SOCIETY OF CHEMISTRY

Fluorescent materials-based information storage

Journal:	*Materials Chemistry Frontiers*
Manuscript ID	QM-REV-10-2019-000607.R1
Article Type:	Review Article
Date Submitted by the Author:	16-Nov-2019
Complete List of Authors:	Wang, Hu; University of Texas at Austin, Chemistry; Zhejiang University, Chemistry Ji, Xiaofan; Zhejiang University, Department of Chemistry Page, Zachery; University of Texas at Austin, Chemistry Sessler, Jonathan; Univ Texas Austin, Chemistry; Shanghai University,

Materials Chemistry Frontiers

REVIEW

Fluorescent materials-based information storage

Hu Wang,[a] Xiaofan Ji, *[,b] Zachariah A Page, *[,a] and Jonathan L. Sessler*[,a,c]

Received 00th January 20xx,
Accepted 00th January 20xx

DOI: 10.1039/x0xx00000x
www.rsc.org/

The third industrial revolution has brought mankind into the information age. The development of information storage materials has played a key role in this transformation. Such materials have seen use in many application areas, including computing, logistics, and medicine. Information storage materials run the gamut from magnetic information storage media to molecular-based information storage materials. Among these, fluorescent-based information storage materials are of particular interest due to their unique properties, including an ability to store information with high levels of security, maintain mechanical stability, and respond to appropriately chosen external stimuli. In this review, we focus on recent advances involving the preparation and study of fluorescent materials-based information storage codes. For organisational purposes, these codes are treated according to the dimensionality of the code system in question, namely 1D-, 2D-, and 3D-type codes. The present review is designed to provide a succinct summary of what has been accomplished in the area, while outlining existing challenges and noting directions for future development.

Introduction

With the advent of the information age, information storage materials are becoming increasingly important.[1-5] Digital information storage networks, ultra-large capacity information transmission, ultra-high-density information storage, and information storage security are topics that are central to the knowledge economy of the 21st century. Materials have a key role to play in these areas. In recent decades, information storage materials have also evolved from bulk materials to thin and ultra-thin layer microstructure materials, and are moving toward optoelectronic information, such as functional integrated chips, organic and inorganic composites, and nanostructured materials.[6-14] Such materials may undergo a sudden change from one state to another under the action of an external stimulus (such as light, heat, or an electric or magnetic field), and can maintain the newly induced state for a relatively long time. By measuring key properties of the materials before and after application of a stimulus, digital information storage in terms of two different states, "0" and "1", becomes possible.

Current information storage materials can be divided into the following categories: magnetic information storage materials, fluorescent information storage materials, and molecular information storage materials. The term magnetic information storage material refers to a type of magnetic material that uses a rectangular hysteresis loop or a change in magnetic moment to store information.[15-27] Such magnetic materials are attractive for memory storage because its two magnetization states can be correlated readily to the binary states “0” and “1” which are readily distinguished by means of magnetoelectric conversion. Fluorescent storage materials differ from magnetism-based systems in that storage and read out of information is dictated by the pattern of the fluorescent material in question.[28-39] Molecular information storage materials are less well explored and are based on the infinite diversity of the molecular space.[40-48] However, for information storage and read out to be facile, there must be two different readily accessible stable (or metastable) states. This review is focused on fluorescent materials-based information storage codes and is designed to summarise recent progress involving their preparation, emissive features, and applications.

Fluorescent materials are attractive for the preparation of information coding systems. One reason is that their fluorescence can only be observed under certain conditions.[49-59] Moreover, the emission of the fluorescent material can be adjusted by changing the excitation wavelength or by controlling the external environment, such as temperature, pH, or chemical. Fluorescent materials can be classified into inorganic fluorescent materials[60-65] and organic fluorescent materials.[66-72] Canonical inorganic fluorescent materials are based on rare earth ions. A number of rare earth complexes display narrow emission bands and are extremely bright. They are also typically quite stable. This has made lanthanide complexes attractive for the construction of full-colour displays. A greater range of organic molecular luminescent materials is known. Most possess conjugated heterocyclic rings and consist of structures that are relatively easy to tailor. For instance, by introducing unsaturated groups, such as an olefin bond or a benzene ring, the nature of the chromophore can be modulated. Not surprisingly, therefore, fluorescent materials are receiving ever-increasing attention and the range of application areas in which they have been applied is seemingly ever-expanding. In addition to being used as dyes, fluorescent materials have been widely applied in many fields, such as organic pigments, optical brighteners, photo-oxidants, coatings, chemical and biochemical analyses, solar traps, anti-counterfeiting labels, drug tracers, and lasers to name but a few. In recent years,

[a] Department of Chemistry, 105 East 24th Street, Stop A5300, The University of Texas at Austin, Austin, Texas 78712, United States; Email: sessler@cm.utexas.edu; zpage@cm.utexas.edu.
[b] School of Chemistry and Chemical Engineering, Huazhong University of Science and Technology (HUST), Wuhan 430074, China. Email: xiaofanji@hust.edu.cn.
[c] Institute for Supramolecular and Catalytic Chemistry, Shanghai University, Shanghai 200444, China.

researchers have used easy processing fluorescent materials,[73-84] including fluorescent nanofibers, fluorescent carbon dots, fluorescent polymers, and fluorescent gels, to prepare a series of information storage codes that store specific information according to their shapes or colours. The colours of these fluorescent information storage codes are only displayed under ultraviolet light, thus allowing the stored information to be protected. In addition, the fluorescent features can be modulated under different stimulation conditions; this makes the stored information potentially dynamic in that it can be modulated in a rational manner. Information storage codes based on fluorescent materials are thus likely to play an ever-increasing role in the fields of information storage and information security. It is this promise that prompts the present review.

Fluorescent information storage codes may be divided into fluorescent 1D codes, 2D codes, and 3D codes according to the dimensionality of the system in question (Fig. 1). Fluorescent 1D codes[73-75] are composed of fluorescent strips and non-fluorescent strips. The pattern of the fluorescent 1D code is only observable under conditions of UV light illumination; this allows for the storage of hidden information and provides for, e.g., very good anti-counterfeiting function. Fluorescent 2D code systems[76-80] record information in horizontal and vertical two-dimensional patterns according to predetermined rules. Again, such code cannot be read under natural light. One the other hand specialized reading devices permit the information to be read upon illumination with UV light. Fluorescent 2D codes have more information storage capacity, a greater degree of confidentiality, and greater error correction than 1D code systems. Fluorescent 3D codes[81-84] are relatively new and add colour to 2D fluorescent codes as a third dimension. The 3D fluorescent code systems reported to date have relied on a matrix of four colours: red, blue, green and black. The information within the code is determined by the shape and colour of the pattern. As typical for fluorescent code systems, 3D codes are decoded under ultraviolet light and typically read out by scanning the pattern as shown schematically in Figure 1.

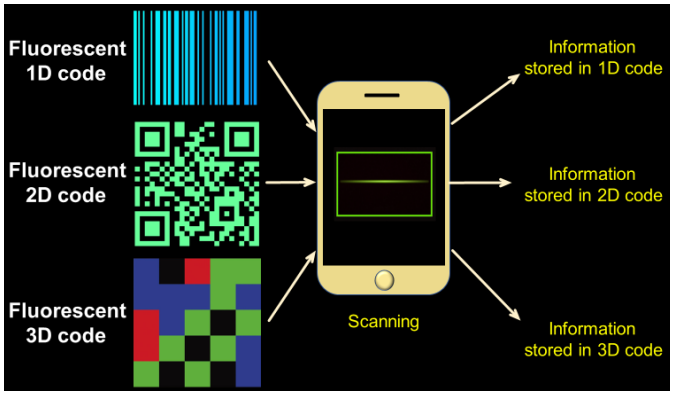

Fig. 1 Schematic diagram of fluorescent 1D-, 2D- and 3D codes.

Fluorescent materials-based 1D information storage codes

1D codes, originated in the 1940s but only became widely popular in the 1980s. As shown in Fig. 2, 1D codes involve a set of regularly arranged bars and spaces.[85-98] "Bar" refers to the portion with low light reflectance, while "space" refers to the portion with higher light reflectance. These bars and spaces express certain information, which can be read by a specific device and converted into binary or decimal information compatible with a computer. Usually each pattern is unique, which has made 1D codes useful for encoding information about items. Such codes are thus near-ubiquitous in the retail sector. 1D code have also been widely used in business, postal, library management, warehousing, industrial production process control, and transportation. In all cases, the correspondence between the 1D code and information is not direct. Rather, it is established through use of an appropriate database. When 1D code data is transmitted to, e.g., a computer, the code data is used to call up stored information. Therefore, the 1D code is only used as an identifier, with its "meaning" only being realized once the associated information is accessed by means of an external database stored within, e.g., a computer server memory bank. On the other hand, 1D codes are inexpensive and easy to use. In fact, a wide range of 1D code systems, including EAN codes, 39 codes, cross 25 codes, UPC codes, 128 codes, 93 codes, ISBN codes, and Kude Bar codes. The 1D codes were scanned using the application software (App) called “Barcode Reader” downloaded to a smartphone, allowing access to the encoded information. The introduction of fluorescent materials into these 1D codes imparts an important additional function. It provides for hidden information that may only be read out under UV light, which adds an extra level of security for information storage, e.g., in the context of anti-counterfeiting. These potential benefits are discussed further below.

Fig. 2 Schematic view of a 1D code.

Fluorescent 1D code-based drug anti-counterfeiting

In the pharmaceutical field, protecting against counterfeit drugs is a concern for manufacturers and patients alike. In order to distinguish manufactured products from counterfeit materials, increasingly drugs are being packaged with specific identifiers, including radio frequency tags, barcodes, watermarks, fluorescent inks, chemical, or biological (e.g., DNA) tags.[99-111] However, such tracking techniques are only effective when the drug in question is not repackaged. Manufacturers usually do not ship drugs directly to hospitals and pharmacies. Usually, drugs are sold to wholesalers or distributors, who then repackage bulk products into unit containers. This is point where counterfeit drugs can enter the legal drug supply chain. In order to circumvent this problem, Smedt and co-authors reported a 1D coded memofiber,[73] which was obtained by electrospinning polymer solutions containing a fluorophore (Fig. 3). The associated information-containing fluorescence pattern is then observed by confocal laser scanning microscopy (Fig. 3).

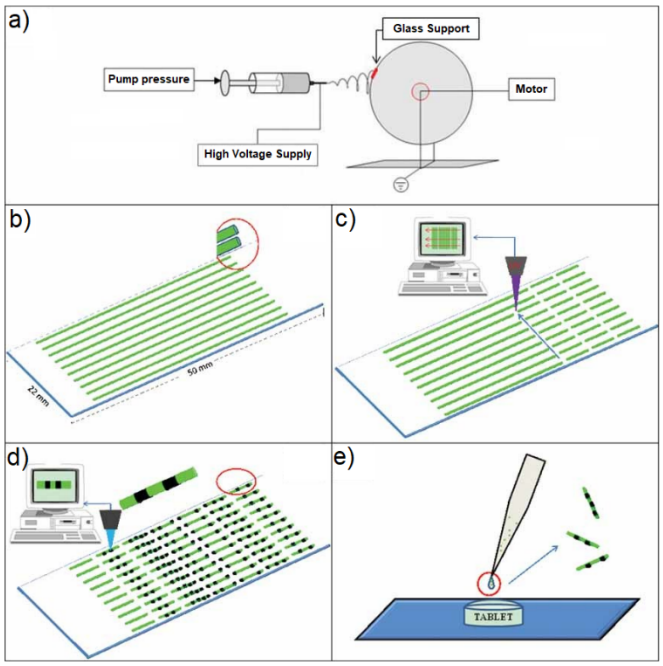

Fig. 3 Synthesis of so-called memofibers. a) Electrospinning setup. b) Electrospinning of polymer fibres on a glass support. c) Cutting of the polymer fibres into fibre pieces by cold ablation. d) Encoding onto the fibre pieces via photobleaching by means of a scanning laser beam. e) Schematic showing the application of a few microliters of a memofiber dispersion on the surface of a tablet. Reproduced with permission from Ref. [73]. Copyright 2010, Wiley-VCH.

The process used to prepare fluorescent memofibers containing a fluorescent 1D code is further shown in Fig. 4. The requisite microfibres were obtained by electrospinning polymer solutions containing a fluorophore. A selected area was photobleached by exposure to a 488 nm laser beam, thus forming microfibers that will provide a 1D fluorescent code under UV illumination. These encoded fluorescent microfibres are then dropped onto the surface of the tablet to produce systems with good long-term stability. The information stored in the 1D microfibre codes can be easily decoded using a basic fluorescence microscope, without removing the microfibers from the tablets. According to the authors, this approach could help curb the proliferation of counterfeit drugs.

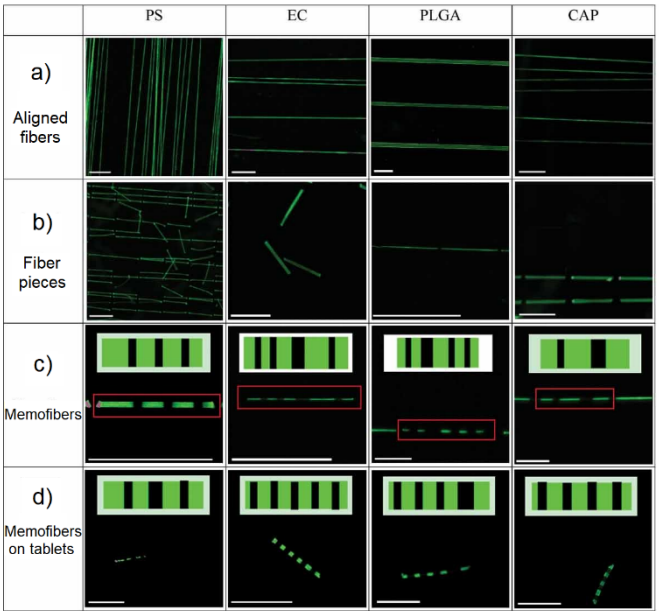

Fig. 4 Fluorescence images of aligned fibre a) and fibre pieces b, c, d) loaded with coumarin-6. The inserts in C and D are barcodes encoded within the fibre pieces and the red rectangles are memofibers. The scale bar is 100 mm. Reproduced with permission from Ref. [73]. Copyright 2010, Wiley-VCH.

Fluorescent 1D code-based biological micro information label

Encoded bead bioassays are receiving increasing attention from researchers and are expected to replace traditional slide-based microarrays.[112-118] Bead-based bioassays offer multiplexing of both probes and samples. At the same time, they have significantly fewer drawbacks associated with mass transport-limited binding of analytes to the immobilized probes. Current methods for making coded beads, involving the injection of polymer microspheres with a predetermined ratio of fluorescent dye mixture, are subject to certain limitations. These include the number of possible codes that can be accessed, difficulties associated with effecting fluorescent read out, as well the potential incompatibility of the beads with the bioassays under consideration. Moreover, the method is not well suited for the manufacture of a large number of uniquely distinguishable beads. Alternative approaches, such as embedding quantum dots in polymer microspheres, raise their own concerns, including the use of toxic materials (e.g., CdS, CdSe, CdTe) in the context of biological assays. It has been proposed that the use of rare earth (RE) ions with silicate glass matrices could provide a viable alternative to these existing approaches. In this context, Lahiri and co-workers described micron-scale glass fluorescent 1D codes,[74] which are composed of different fluorescent materials containing rare earth ions (Fig. 5). These fluorescent 1D codes can be easily identified by using UV lamps and optical microscopes. The use of RE doped glass provides fluorescent 1D codes characterized by relatively narrow emission bands, high quantum efficiencies, and good compatibilities with other common fluorescent labels and most laboratory solvents. Using this approach a model DNA hybridization assay consisting of what was termed ‘‘micro 1D codes’’ by the authors was described. In this model, bar codes with different fluorescent colours correspond to specific biological information.

The large number (> 1 million) of possible combinations could make this fluorescent 1D code approach attractive for use in both bioassays and general encoding applications.

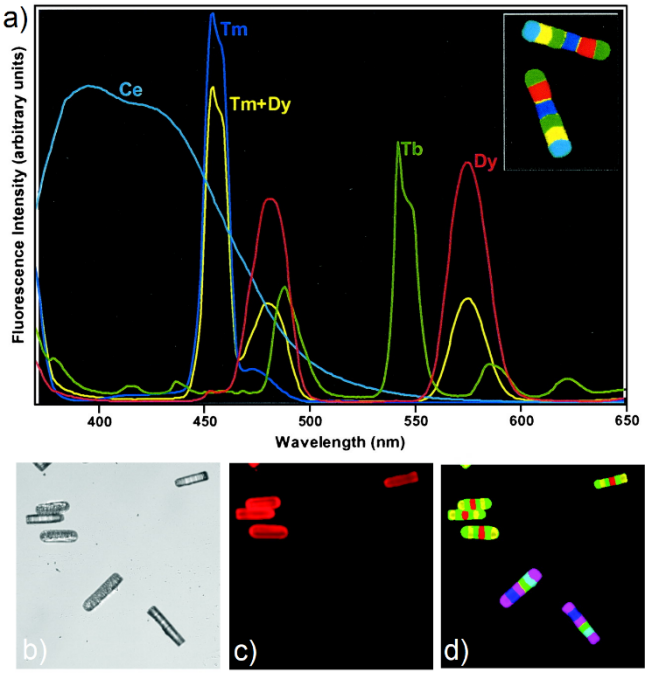

Fig. 5 a) False-colour image of two 100 × 20 µm barcodes (inset) and corresponding fluorescence spectrum barcode elements. The same colour scheme is used for the spectra and the image [e.g., the yellow band in the barcode corresponds to the yellow (combination Tm + Dy) line spectrum]. Fluorescence false-colour images of 1D code particles used in a DNA hybridization assay using Cy3-labeled DNA. b) ''White light'' image. c) Cy3 channel image. d) RE images obtained by using a 420-nm long-pass filter. Reproduced with permission from Ref. [74]. Copyright 2003, National Academy of Sciences (USA).

Fluorescent 1D code-based encrypted label

Solid-state materials with photoluminescent features have been widely applied in many fields, including for OLED development,[119-121] data recording and storage,[122,123] dye lasers,[124] and security printing.[125,126] Stimuli-responsive photoluminescent materials are expected to be useful in the next generation of security printing. Nevertheless, it remains a major challenge to develop wide-spectrum tuneable photoluminescent solid-state materials that give rise to multiple fluorescent emission bands. Stoddart and co-workers reported a hetero[4]rotaxane (Fig. 6), which was isolated as an unexpected side product during the synthesis of heterorotaxane from CB[6], γ-CD, and two fluorescent precursors (derived from pyrene and a diazaperopyrenium (DAPP) dication, respectively).[75] The fluorescence emission of this hetero[4]rotaxane in the solid state could be tuned rapidly and reversibly over a wide range (~100 nm) of wavelengths as a result of stimuli-responsive aggregation and de-aggregation processes. Moreover, this hetero[4]rotaxane was found to aggregate at high concentrations to form supramolecular oligomers. Under conditions of aggregation the initial narrow emission band at 510 nm was replaced by a broad, featureless band around 610 nm, leading the authors to infer that either excimers (DAPP homodimers) or exciplexes (pyrenyl-DAPP heterodimers) were being formed in the excited state. Heating the aggregated forms led to reversion back to the disassociated species. The authors applied this reversible fluorescent supramolecular construct to the preparation of fluorescent inks, which in turn were used to prepare a series of patterns. These patterns are difficult to visualize under natural light, but became readily apparent under conditions of UV light illumination. A 1D code created from this material was produced that could be read by a smartphone. This research could represent a new way to encrypt and protect information.

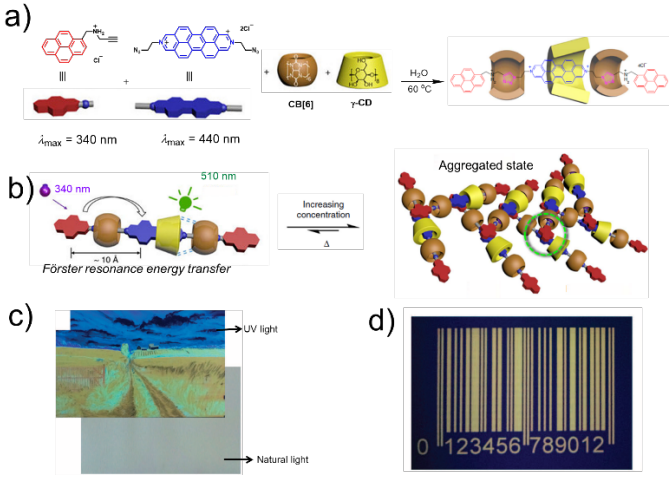

Fig. 6 a) Formation of hetero[4]rotaxane. b) Graphical representation of the aggregation of monomers in response to changes in concentration or temperature. c) Fluorescent image printed using an inkjet printer under conditions of UV and natural light illumination. d) photograph of a UV 1D code produced from the hetero[4]rotaxane system under UV light irradiation. Reproduced with permission from Ref. [75]. Copyright 2015, Nature Publishing Group.

Fluorescent materials-based 2D information storage codes

So-called 2D codes record data information in a black and white pattern maintained within a plane. These are thus specific geometric patterns defined by horizontal and vertical coordinates.[127-130] Black and white rectangular patterns have been used to provide 2D codes. These, in turn, could be scanned using the App "QR Code Reader" downloaded to a smartphone in order to read out the encoded information (Fig. 7). In contrast to 1D codes, in 2D codes, data is recorded in both the length and the width of the individual pattern elements. The resulting increase in information density allows "0" and "1" bit streams to be encoded. Moreover, the vast number of geometric shapes that can be defined within a 2D code system, allows direct storage of numerical data. Thus, in the case of 2D codes, photoelectric scanning allows automatic information processing without resorting to a database. Moreover, 2D codes can incorporate "positioning points" and "fault tolerance mechanisms" that are not available to 1D codes. In favorouble

circumstances, this allows 2D codes to be read even if the entire barcode is not recognized or the barcode is defaced. Not surprisingly, 2D codes have enjoyed tremendous commercial success, especially in the high-tech industry, data storage, transportation, wholesale, and other industries. As in the case of 1D systems, 2D codes made from fluorescent materials offer the advantages of providing anti-counterfeiting capabilities. In addition, fluorescent materials can allow for the self-healing of 2D code systems. As detailed further below, these and other attributes lead to the prediction that fluorescent materials-based 2D codes could expand the range of applications and allow for new advances in information science.

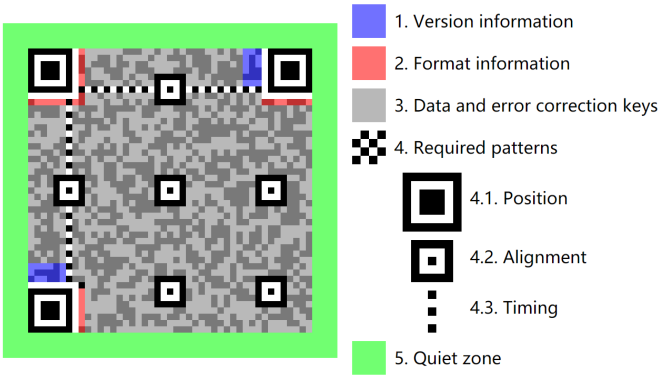

Fig. 7 Schematic illustration of the component units that make up a typical 2D code system.

Fluorescent 2D code-based massive drug anti-counterfeiting label

As noted above, eliminating counterfeit drugs is an ongoing challenge.[101-105] To go beyond what has been achieved using 1D fluorescent codes, Park and co-workers explored the use of 2D codes in the context of drug anti-counterfeiting (Fig. 8).[76] Here, an optofluidic maskless lithography (OFML) system was used to produce a 2D code on a polymeric micro taggant. This OFML system allowed the high-resolution and high throughput fabrication of polymer microparticles with arbitrary shapes (Fig. 8C). UV light, reflected off the 2D code pattern on a digital micromirror device (DMD), was projected onto the microfluidic channel, into which a photocurable polymer solution (poly(ethylene glycol) diacrylate) had been introduced. 2D-coded micro taggants were then generated via the photopolymerization of poly(ethylene glycol) diacrylate through a single UV exposure. The resulting fluorescent 2D information storage code not only allowed for simple drug identification, but also provided a means to store a large amount of drug-releated information. The information carried by these 2D codes could be read using a simple smartphone 2D code reader application. This allowed the drugs in question to be tracked more effectively. Importantly, since 2D codes provide for good inherent error correction, partial damage of the drug substance was not found to affect adversely either the storage or read out of the encoded information. This technology could thus emerge as one that helps prevent the proliferation of counterfeit drugs.

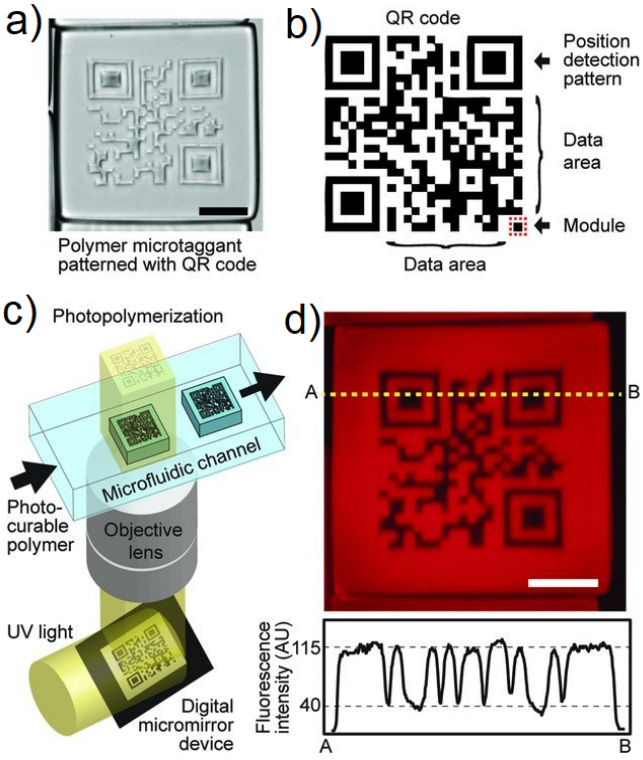

Fig. 8 a) Microscope image of 2D code (scale bar: 200 μm). b) Structure of the 2D code. c) 2D code-containing polymer microtaggant prepared using an optofluidic maskless lithography (OFML) system. d) Fluorescence microscope image of the 2D-coded micro taggant and the line profile (A–B) of the fluorescence intensity (scale bar: 100 μm). Reproduced with permission from Ref. [76]. Copyright 2012, Wiley-VCH.

Fluorescent 2D code-based information security pattern

Fluorescent carbon dots (CDs) are attracting increasing attention due to their highly stable fluorescence, good resistance to light and chemical degradation, low toxicity, and excellent biocompatibility.[131-136] These attributes make CDs attractive for use in a wide range of application areas, including biomedical imaging, photocatalysts, sensors, and optoelectronic devices. There are many methods for preparing CDs, including electrochemical synthesis, microwave/ultrasonic preparation, hydrothermal/acid oxidation routes, arc discharge, laser ablation, and plasma treatment. The raw materials for the preparation of CDs include both traditional chemicals (citric acid monohydrate, carboxylates and carbohydrates) and renewable resources (gas soot, soybeans, orange juice, and grass). In work relevant to the preparation of fluorescent 2D codes, Chen and co-workers recently presented a simple, low-cost, and green method to obtain highly fluorescent CDs from a series of plant leaves by pyrolysis (Fig. 9).[77] The resulting fluorescent CD were found to be responsiveness to Fe^{3+} ions and could be used to prepare patterns attractive for anti-counterfeit applications.

Fig. 9 Schematic synthesis of CDs from pyrolysis of plant leaves and the photoluminescence enhancement by plasma and microwave irradiation. Also shown are photographs of the corresponding samples under ambient light and UV illumination. Reproduced with permission from Ref. [77]. Copyright 2013, The Royal Society of Chemistry.

As shown in Fig. 10, Chen and co-workers used inkjet printing technology to print fluorescent CDs into patterns or 2D codes carrying information. An electric field was applied to squeeze the materials, which generated a pressure pulse and served to force ink droplets (fluorescent CDs) out of the nozzle; this allowed the printing of patterns on paper substrates. It is worth noting that the pattern solution printed from the CD is not visible under ambient light, but only under conditions of UV light illumination (Fig. 10b). As shown in Figs. 10c and 10d, a fluorescent pattern of a plum blossom and a 2D code may be formed readily on the paper substrate. The ambient light invisible and UV-visible properties of this material could allow for their application in the area of anti-counterfeiting.

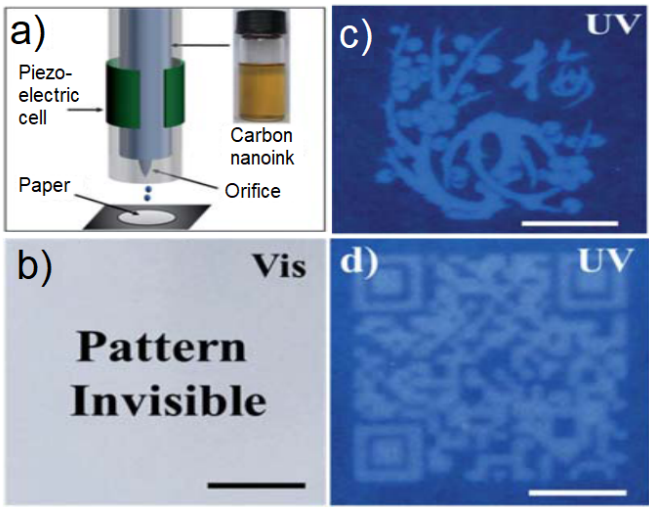

Fig. 10 a) Scheme of piezoelectric inkjet printing. Inset: the as-prepared fluorescent carbon ink. b) Photograph of the fluorescent pattern by inkjet printing. Photograph of the fluorescent pattern under UV light: c) Plum blossom and d) 2D code. The scale bar is 1 cm. Reproduced with permission from Ref. [77]. Copyright 2013, The Royal Society of Chemistry.

Fluorescent 2D code-based information storage organogel

With the rapid development of network information technology, information security is evolving as an ever greater concern. In fact, ensuring the security of 2D codes and their associated information represents an increasingly important issue within the context of information science. Avoiding damage to 2D codes represents another challenge. Therefore, it is desirable to develop protected codes with greater durability and security. Maintaining the large colour contrast would be desirable in such putative systems since it is expected to facilitate the rapid read out of encoded information.[137-139] Recognizing this need Huang and co-workers reported a hydrogen bond-based approach to preparing white-light-emitting fluorescent polymeric gels that involved the aggregation of a single fluorescent chromophore (Fig. 11).[78] In this system, a pyridinium salt monomer, which is a donor–acceptor molecule, is used since it emits intense white light upon aggregation. The resulting gel has features that make it attractive for constructing intelligent information display/storage devices. In fact, a protected 2D code was fabricated from Huang's white-light-emitting fluorescent supramolecular gel. As expected for a fluorescent code system the stored information could not be read out under natural light conditions but was fully accessible under a UV lamp. Of particular interest is the fact that, as the result of the dynamic nature of the system, the supramolecular polymer gel and the resulting 2D code were shown to have self-healing abilities. In fact, an intentionally damaged 2D code was prepared whose information could not be read out under UV light irradiation. Interfacial self-assembly of the gels (resulting from reformed hydrogen bonding interactions; cf. Fig. 11) then allowed recovery of the originally protected information.

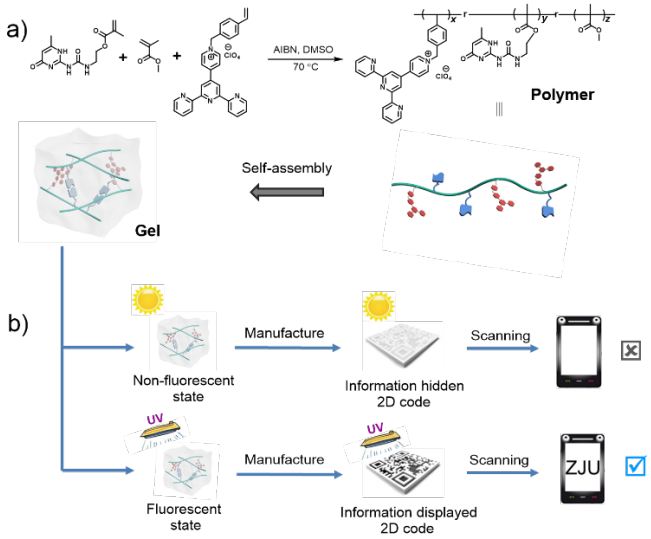

Fig. 11 a) Controlled self-assembly that allows formation of a white-light-emitting fluorescent supramolecular polymer gel *via* intermolecular hydrogen bonding. b) Cartoon representation of data recording and data security protection of a 2D code constructed using this gel. Reproduced with permission from Ref. [78]. Copyright 2017, the Royal Society of Chemistry.

Fluorescent 2D code-based biometric label

Generally, code tag systems are fabricated by incorporating different organic fluorescent tags in specific ratios, providing a limited number of unique codes.[140-143] Another type of fluorescence encoding involves photobleaching of the fluorescent material to create a master. This method is also known as *active encoding*. However, this method also suffers from certain limitations, such as negative contrast and photobleaching of the fluorescent portions of the ensemble. In an effort to overcome some of these recognized issues, Sels and co-authors reported a new type of optically encoded microcarrier that was based on silver-exchanged zeolite crystals that were then subject to a two-photon activation process with near-infrared light.[79] During this process, the silver cations in the crystal are photochemically reduced to local silver clusters. Due to the positive contrast imaging and the brightness and stability of the resulting emissive silver clusters, very low write resolution (down to the diffraction limit) and excellent readability are obtained. Excellent 3D resolution allowed creation of an advanced matrix code (e.g., a 2D code) inside a single zeolite microcarrier (Fig. 12). Interestingly, a number of high resolution encoding and decoding strategies proved compatible with these silver zeolite microcarriers when they were suspended in aqueous solution. The authors thus proposed that they could see utility in a variety of biomarker applications.

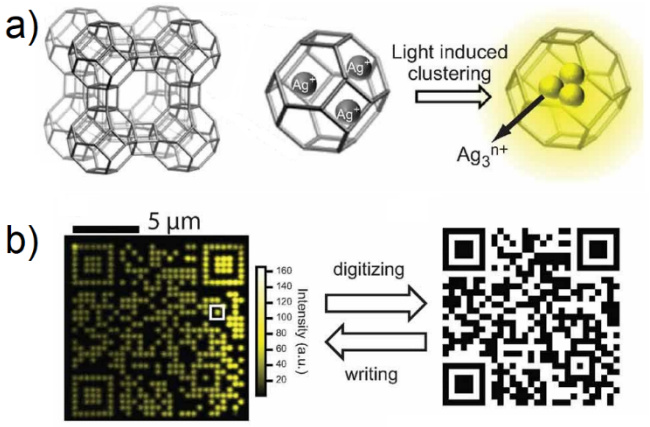

Fig. 12 a) Schematic illustration of silver zeolite. b) Fluorescence image of a silver zeolite 2D code (left) and the corresponding original image (right). Reproduced with permission from Ref. [79]. Copyright 2012, Wiley-VCH.

Fluorescent 2D code-based lithographic information storage hydrogels

A number of jellyfish are notable for their switchable bioluminescence on/off characteristics. This capability has inspired the design of hydrogels with adjustable fluorescence. Typically, this has been done by incorporating a chromophore into a hydrogel matrix.[144-146] Regulation of the fluorescence is then achieved by controlling the properties of the chromophore. In this context, hydrogels with white light emission capabilities are particularly attractive. These systems are characterized by the presence multiple emission peaks, which do not necessarily respond in concert to the same stimulus. This allows for the construction of fluorescent hydrogel-based chemical sensors with improved sensitivity. Wu and co-workers reported a white light emission (WLE) hydrogel containing a single chromophore that was prepared *via* a one-pot micellar copolymerization of 4′-(*N*-vinyl benzyl-4-pyridinyl)-2,2′:6′,2″-terpyridine perchlorate and acrylamide (Fig. 13).[80] The resulting transparent hydrogel showed strong white fluorescence under UV light irradiation. The fluorescence spectrum of the gel is dominated by two emission features centred around 450 and 570 nm. These bands correspond to the monomer and dimer forms of the chromophore, respectively. The CIE coordinate values of the white light fluorescence was (0.333, 0.335). The monomer and dimer have distinct optimal excitation wavelengths, λ_{ex}. Therefore, the fluorescent behaviour of this gel was found to depend on the λ_{ex}. Furthermore, the monomer-to-dimer transformation of the chromophore could be triggered by heating or photo-irradiation, allowing the fluorescence of the hydrogel to be tuned from blue to white and then to yellow. Photo-irradiation allowed photolithographic patterning of the hydrogel giving rise to patterns that are transparent under ambient light conditions, but fluorescent (and hence readily visible) when irradiated with ultraviolet light (Fig. 14). The fluorescence could also be switched off by exposure to Cu^{2+} ions. It was proposed that the adjustable fluorescence and patterning properties of this single chromophore-based WLE hydrogel could make it particularly useful in the secure information storage arena.

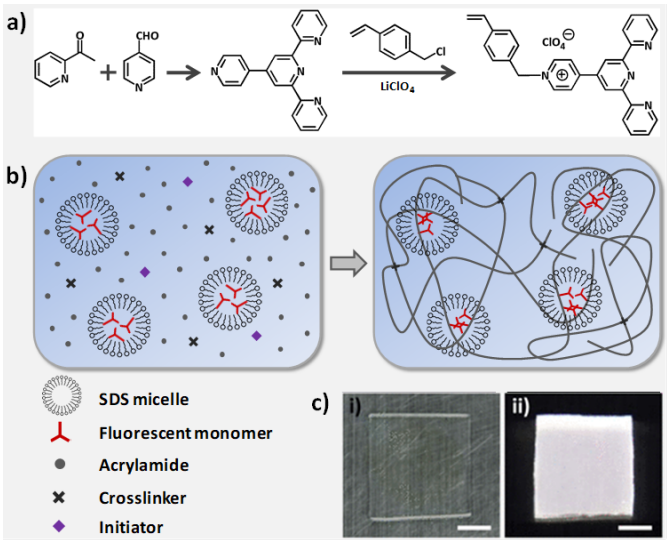

Fig. 13 a) Synthesis of a chromophore monomer. b) Preparation of fluorescent hydrogel by micellar copolymerization. Monomer and dimer forms of the fluorescent units coexist in the hydrogel, giving rise to high- and low-energy emission bands, respectively. The net result is white light fluorescence under UV excitation. c) Photos of the hydrogel under (i) ambient light and (ii) UV light irradiation. Scale bar: 5 mm. Reproduced with permission from Ref. [80]. Copyright 2018, The American Chemical Society.

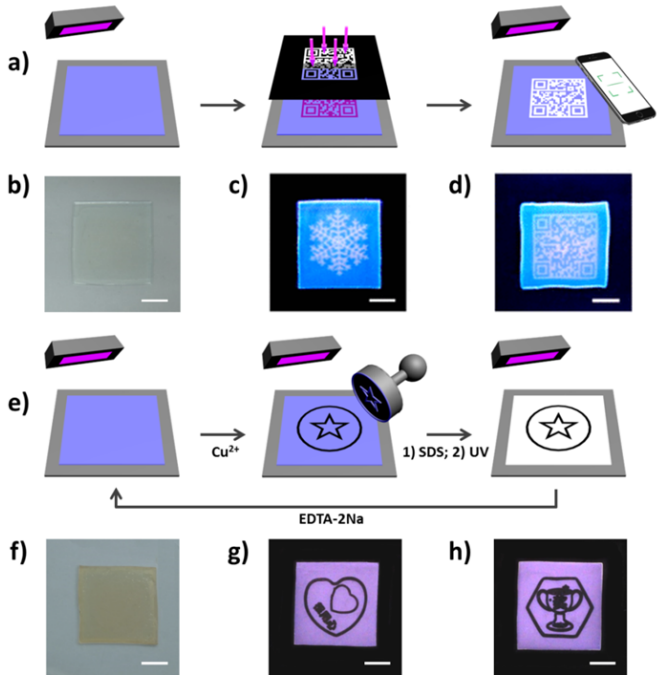

Fig. 14 a) Schematic for patterning fluorescent hydrogel by photolithography. The blue fluorescent gel was irradiated under UV light through a photo mask, resulting in white fluorescence at the exposed regions. b–d) Photos of the patterned hydrogel under b) ambient light and c, d) UV light (different patterns). e) Schematic for patterning the hydrogel by wet stamping. A stamp soaked with Cu^{2+} ions was used to pattern the blue form of the fluorescent gel by selectively quenching the fluorescence. The emissive features of the gel could then be restored by using ethylene diamine tetraacetic acid disodium salt (EDTA-2Na) to extract the Cu^{2+} ions. f–h) Photos of the patterned hydrogel under f) ambient light and g, h). conditions of UV illumination (two patterns on one gel). Scale bar: 1 cm. Reproduced with permission from Ref. [80]. Copyright 2018, The American Chemical Society.

Fluorescent materials-based 3D information storage codes

The 3D codes rely on colour to provide the third "dimension" of information storage. Such systems, also referred to as colour codes, were originally developed on the basis of traditional black and white 2D codes. Early systems thus consisted of an n × n matrix containing individual blocks with one of four colours, red, blue, green, and black.[147] The outer frame of the matrix is enclosed by black lines, while a white background outside the black border provided an outer frame. In contrast to traditional 2D codes, 3D colour code systems need not encrypt all the information with the code. Rather, they can be used as "pointers" to site, such as a server address, where the desired information is stored. Operationally, existing material-based 3D codes have relied on mobile phone reader applications to record and send code-derived index information to a server. After verification, the index information is uploaded to the server, converted into a URL address which is transferred to the corresponding content server, thereby allowing the information to be displayed on the phone (Fig. 15). The 3D code could be scanned using the App "COLORCODE" downloaded to a smartphone in order to read out the encoded information. Due to the special identification method (i.e., the information is read out by judging the colour pattern of the n x n matrix), 3D codes have relatively high resistance to deformation.

While a number of colour code strategies can be conceived, fluorescent materials are particularly well suited for preparing 3D codes. They are easy to manipulate and often endowed with self-healing characteristics. Moreover, stimuli responsive fluorescent materials can be used, which allows controlled changes in the information stored by the 3D codes under different conditions. The resulting dynamic information storage capability is difficult to replicate in simpler 1D code and 2D code systems. Not surprisingly, fluorescent 3D codes are attracting attention, particularly where a high degree of confidentiality is required or anti-counterfeiting measures would be desirable.

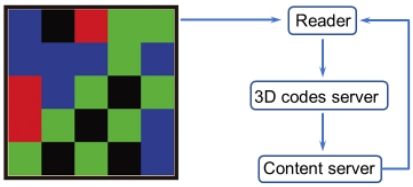

Fig. 15 The process used to read information from a 3D colour code.

Fluorescent 3D code-based dynamic information grid

As noted above, information codes have become all but essential for manufacturers, suppliers, and consumers alike.[148,149] Although the amount of information carried by traditional information codes is gradually expanding (1D, 2D, and 3D codes), existing product information codes are generally static; the information they store and provide cannot be altered after they are created. The ability to transform or adjust coded information, rather than just storing it in a static form, could bring increased benefits to both producers and consumers. Sessler and co-workers reported an approach to generating fluorescent 3D colour codes. These systems were constructed by using three fluorescent (blue (G1), green (G2), and red (G3-1, G3-2)) hydrogels containing both tetracationic receptor–anion recognition motifs and gel-specific fluorophores.[81] These different hydrogels were then bonded together by physical adhesion to produce a 5x5 grid (Fig. 16). The resulting three-dimensional code allowed for a number of key information-related functions, including data masking, demasking, and erasing, as well as dedicated conversion to different encoded forms. For example, code B could be converted to code A (storing other information) by replacing one of the gel components within the grid. It was also shown that when one of the constituent gel components was chemically responsive (to ammonia in this initial study), the resulting grid pattern, code C, could be converted to the original code A by chemical exposure. The ability to convert encoded information produced by these gels to a different form by either physical action or by exposure to a chemical stimulus offers the possibility of transitioning current commercial codes to ones with dynamic

capabilities. Also attractive is the fact that this demonstration relied on an ostensibly biocompatible hydrogel, meaning that these codes could potentially be used as wearable information-containing materials.

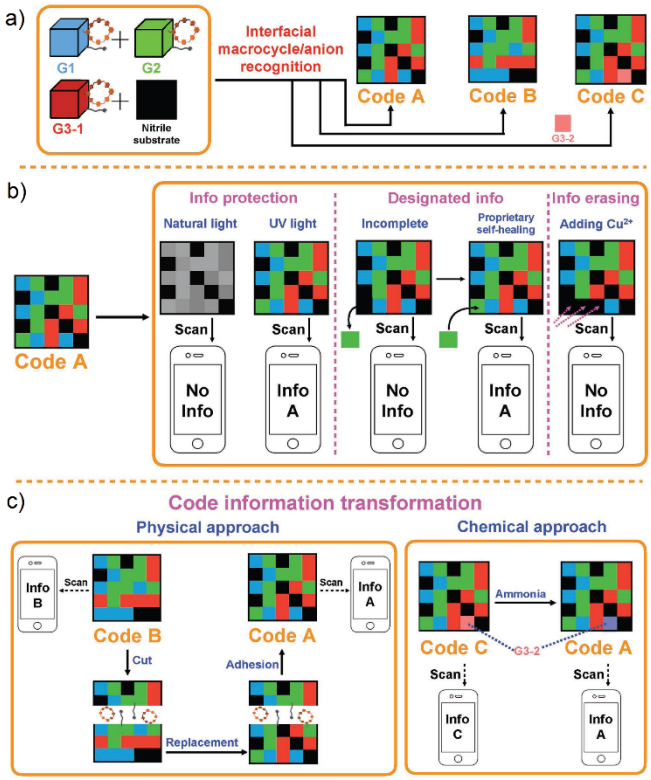

Fig. 16 Cartoon representations of: a) Formation of 3D colour codes made up of hydrogels G1, G2, and G3 (G3-1 and G3-2). b) Information protection, designated information read out, and information erasing of code A. c) Transformation of encoded information through physical action and chemical exposure. Reproduced with permission from Ref. [81]. Copyright 2018, Wiley-VCH.

In recent years, many advances have been made in the area of anion recognition and sensing. [150-156] Many strategies have been used to signal the presence of anions, such as monitoring chemical shift changes *via* NMR spectroscopy, UV/vis spectral analyses, fluorescence emission spectroscopy, and mass spectrometry. However, most of these strategies require access to laboratory instrumentation, which greatly limits their practical utility in the field. Building upon their initial fluorescence 3D code work summarised immediately above, Sessler and co-workers reported a double layer 3D code made from eight fluorescent polymeric gels; these allowed direct recognition of the chloride anion using a smart phone.[82] As shown in Fig. 17, a fluorescent pattern (code D) was constructed from gels containing calix[4]pyrroles (C4P)/imidazolium-F^- anion recognition motifs. This pattern be read out by a smart phone as a 3D colour code (i.e., info D). Gels containing C4P/imidazolium-Br^- anion recognition motifs were used to construct an array (code E) that could be read as info E. Using these two grid-type pattern arrays, a two-layer code system was made; this was done by adhering code E to the surface of code D. This annealing results in code E being the top layer and the only one that is readily visible. It could be read out with little appreciable interference from code D. Treating the overall construct with a Cl^- anion source resulted in delamination of the top layer (code E) revealing the bottom layer (code D), which could then be read out. This code system was thus specific to chloride ions. This sensing strategy, which does not rely on precise molecular recognition effects, could represent a new application for complex soft materials.

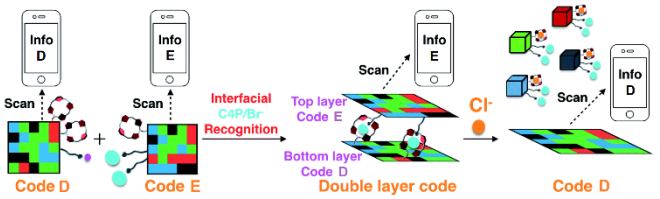

Fig. 17 Formation of a double layer code construct stabilized via presumed interfacial anion-receptor interactions involving the recognition elements present in codes D and E. Also shown is the proposed Cl^- anion induced delamination and encoded information release-based sensing mechanism that allows for chloride anion recognition. Reproduced with permission from Ref. [82]. Copyright 2018, The Royal Society of Chemistry.

Phosphorescent 3D dynamic codes

Subsequent to the initial Sessler report on fluorescent 3D codes, a number other groups reported materials-based colour codes.[83,84,172] Much of this work is very recent and it appears that this is an area that is attracting considerable attention. One approach is based on phosphorescent materials that emit for hours following photo-irradiation.[157-159] While relatively few in number, phosphorescent materials are known to give rise to different outputs (i.e., emission bands and colours) when exposed to appropriately chosen stimuli. For practical applications, such as information encryption, sensor development, and anti-counterfeiting, dynamic phosphorescent materials must meet the following criteria: (i) Display broad-spectrum emission; (ii) possess dynamic characteristics with the nature of the emitted light being readily fine-tuned via exposure to external stimuli; (iii) be relatively robust. Recently, Ge and co-workers reported a simple method for fabricating light-tuneable, full-colour luminescent materials based on dynamic trichromatic emitters (Fig. 18).[83] These trichromatic emitters are $SrAl_2O_4:Eu^{2+},Dy^{3+}$, $CaAl_2O_4:Eu^{2+},Nd^{3+}$ and $Ca_{0.25}SrS_{0.75}:Eu^{2+}$. By simply mixing these emissive constituents together, a pattern was obtained that could be observed under UV-visible illumination. Adjustments to the individual emissive elements could be achieved by varying the constituent ratio or by changing the excitation wavelength. The authors prepared a three-dimensional (3D) code, which could be read using a smartphone by preparing and arranging individual elements made up from these trichromic emitters. The resulting 3D code pattern could only be read after being illuminated by a UV-visible lamp. Moreover, by varying the external conditions, such as by exposure to ammonia, the information embodied in the 3D code could also be changed. It was thus proposed that this dynamic phosphorescent system

may find utility in the areas of information storage, encryption, and stimulus-based modification.

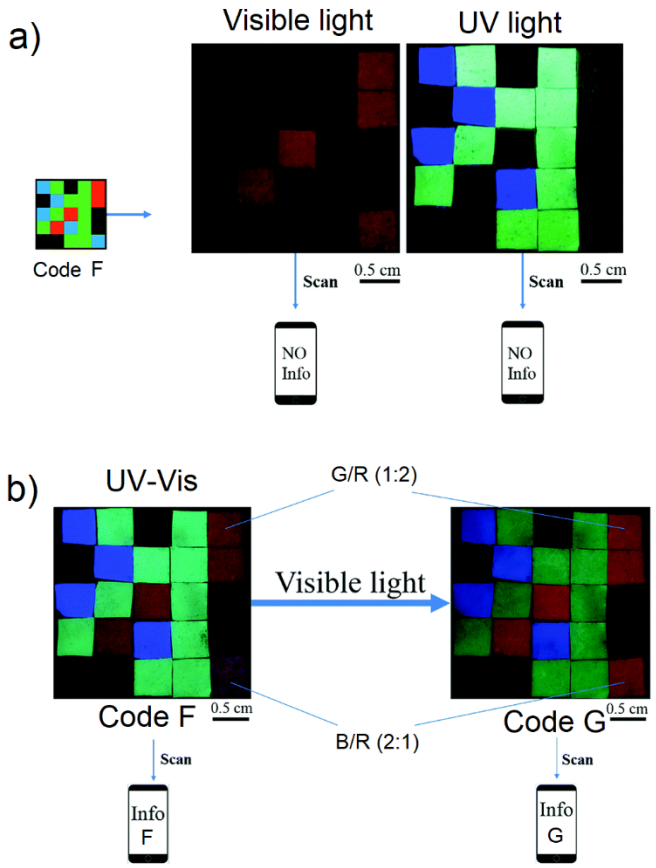

Fig. 18 a) Photographs of the read out of information inherent in code F, a pattern made up by the assembly of individual domains of trichromic materials on a supporting black nitrile substrate and b) photographs of the code information transformation from info G to info F produced upon exposure to ammonia vapor. Reproduced with permission from Ref. [83]. Copyright 2018, The Royal Society of Chemistry.

Fluorescent 3D codes based on self-healing materials

Self-healing materials have attracted attention across a number of application areas because of their ability to recover spontaneously both function and structure after damage.[160-165] Self-healing gels constructed by means of dynamic covalent or non-covalent interactions have attracted increasing interest, including in the construction of fluorescent 3D codes as noted above. However, these constructs, and indeed all fluorescent-based systems, are highly dependent on the performance of the fluorophore. Many classic fluorophores suffer from limitations, including poor photo-stability and induced quenching at higher concentrations. Recently, fluorescent materials displaying aggregation-induced emission (AIE) have been developed in an effort to overcome the so-called aggregation-caused quenching (ACQ) effect that plagues many traditional fluorophores. Recently, Tang and co-authors reported the use of fluorescence self-healing gels with turn-on AIE capability to create 3D codes (Fig. 19).[84] Using this approach, it proved possible to monitor the microscopic self-healing process of the gel, as well as the production of several fluorescent 3D codes with anti-counterfeiting capabilities. These self-healing 3D codes are attractive for their scalability, wear resistance, reusability, and versatility.

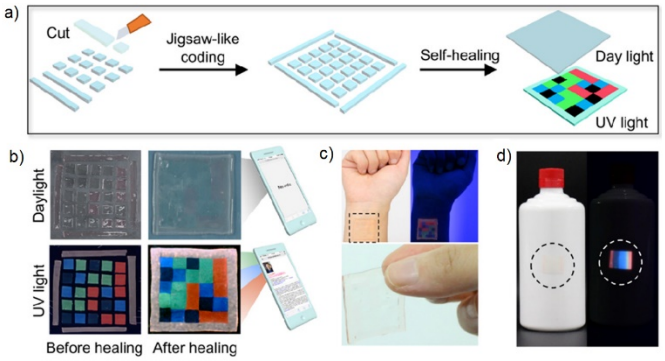

Fig. 19 a) Schematic illustration of the procedure used to create a 3D fluorescent code *via* self-healing. b) Photographs of the fluorescent 3D code arrays taken before and after self-healing. c) Illustration showing that the 3D codes of parts a) and b) are compatible with skin and may be readily worn, and d) anti-counterfeit fluorescent bar code that may be applied to, e.g., an alcoholic beverage container and its visualisation under ambient and UV light. Reproduced with permission from Ref. [84]. Copyright 2019, The American Chemical Society.

Fluorescent materials have been widely used in many fields[166-171] and have proved critical to the development of 3D code systems. The resulting patterns are typically only visible under UV light. While this is useful for encryption and anti-counterfeit measures, it also limits the utility of the systems under conditions where UV illumination is not practical. Recently, Zhao and co-workers reported a light-triggered luminescence ON-OFF switchable hybrid hydrogel (Fig. 20).[172] The hydrogel was constructed via polymerization of acrylamide while incorporating diarylethene photochromophore and a luminescent lanthanide complex. The diarylethene ring within the polymer could undergo "open" and "close" isomerization upon alternating between UV and visible light irradiation. Upon photo-excitation of the material containing the closed form of the diarylethene ring, fluorescence resonance energy transfer to the lanthanide complex occurs. Based on this hybrid hydrogel, the authors constructed a 3D information code. The code could be read out under a 254 nm UV lamp. After exposure to 300 nm UV light, the luminescence of the hydrogel was quenched and the encoded information was effectively erased. After exposure to visible light (> 450 nm) the fluorescence was restored and the information encoded within the hydrogel could be read out once again. Thus, through a simple process involving light illumination, the information inherent within the 3D code could be encrypted and decrypted. This research thus marks a further step towards the development of smart materials.

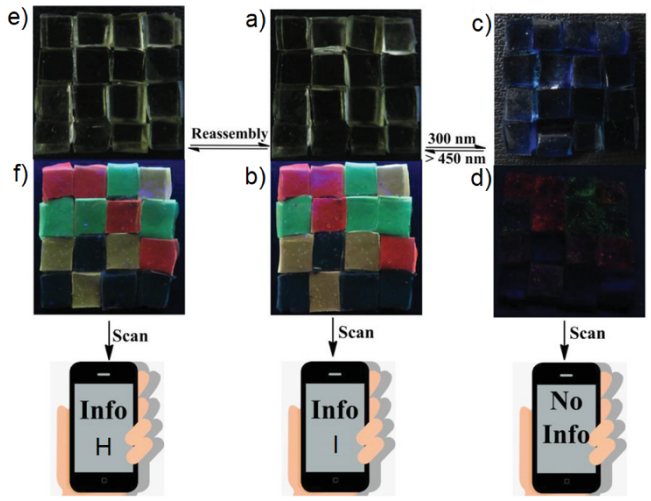

Fig. 20 a,c) Photographs of a pattern (code H) made up from an ensemble containing red, green, and yellow hydrogels on a black substrate under ambient light before and after irradiation with 300 nm UV light. b,d) Under these conditions, the information could either be read out or masked. e,f) Photographs showing the transformation of code H into code I under amibient light and 254 nm UV light by means of a reassembly strategy. The hydrogels were all assembled on the same substrate. Photographs shown in panels a), c), and e) were all taken under daylight, whereas photographs of b), d), and f) were taken under 254 nm UV light. The size of each hydrogel block element within the overall code pattern is 0.5 cm × 0.5 cm × 0.2 cm. Reproduced with permission from Ref. [172]. Copyright 2019, Wiley-VCH.

Conclusions

In this review, we summarise recent progress in the field of fluorescent materials-based information storage. Depending on the dimension, fluorescent materials can be used to fabricate 1D, 2D, and 3D information storage codes. They have unique properties compared to conventional codes. Firstly, the introduction of fluorescent materials greatly improves the anti-counterfeiting ability of information storage codes. The fluorescence information storage code can only be displayed under UV light and is invisible under ambient light, which allows the information it carries to be displayed when needed, but otherwise hidden. Secondly, some fluorescent materials with unique mechanical properties greatly improve the information stability of the information storage code. For example, self-healing features can be introduced into the fluorescent materials used to make up a number of codes. Thirdly, fluorescent materials that are responsive to naturally occurring external stimuli have enabled the preparation of interconvertible storage codes. These could represent the vanguard of a new level of development, where traditional static information coding gives way to dynamic information storage, manipulation, and read out. We thus believe that luminescent materials will allow for further advances in a number of areas related to information technology.

Although the development of fluorescent materials-based information storage has made great progress, there are still issues that need to be addressed if their full promise is to be realized. For example, the information storage permitted by fluorescent 1D codes is limited. Moreover, the information stored is difficult to recover if the code system is damaged. Increasing information storage density and improving the fault tolerance represent opportunities for development in the context of fluorescent 1D codes. Currently, complex patterns are an inherent feature of fluorescent 2D codes. This complexity is not conducive to large-scale manufacturing. Therefore, developing 2D codes that are easier to fabricate would fill a recognized need. So far fluorescent 3D codes have been based on 5 × 5 grids. In order to increase the information stored, it will be necessary to extend the number of building blocks from 5 × 5 to n × n (where n ≥6). Adding yet another dimension to produce nD codes (n ≥ 4) via the introduction, e.g., of a temporal response element, could further increase the level of stored information for any given system and provide greater control over the read out of that information. In addition, introducing additional stimuli responsive features could make the fluorescent codes more useful in the context of sensor development for reading out environmental-based changes; this would be useful for monitoring both changes in patient physiology and various industrial processes. We are confident that these challenges can be met and, as a consequence, the field of fluorescent materials-based information storage has a bright future.

Conflicts of interest

There are no conflicts to declare.

Acknowledgements

Support from the National Science Foundation (CHE-1807152 to J.L.S.) and the Robert A. Welch Foundation (F-0018 to J.L.S. and F-2007, Z.A.P.) is gratefully acknowledged. X.J. thanks initial funding from the Huazhong University of Science and Technology for partial support of this work.

Notes and references

1. W. Tittel, M. Afzelius, T. Chaneliére, R. L. Cone, S. Köll, S. A. Moiseev and M. Sellars, *Laser Photon. Rev.*, 2010, **4**, 244–267.
2. M. P. Hedges, J. J. Longdell, Y. Li and M. J. Sellars, *Nature*, 2010, **465**, 1052–1056.
3. A. I. Lvovsky, B. C. Sanders and W. Tittel, *Nat. Photon.*, 2009, **3**, 706–714.
4. C. Simon, M. Afzelius, J. Appel, A. Boyer de la Giroday, S. J. Dewhurst, N. Gisin, C. Y. Hu, F. Jelezko, S. Kröll, J. H. Müller, J. Nunn, E. S. Polzik, J. G. Rarity, H. De Riedmatten, W. Rosenfeld, A. J. Shields, N. Sköld, R. M. Stevenson, R. Thew, I. A. Walmsley, M. C. Weber, H. Weinfurter, J. Wrachtrup and R. J. *Young, Eur. Phys. J. D*, 2010, **58**, 1–22.
5. I. Usmani, M. Afzelius, H. de Riedmatten and N. Gisin, *Nat.*

Commun., 2010, **1**, 1–7.
6. R. A. Bissell, A. P. de Silva, H. Q. M. Gunaratne, P. L. M. Lynch, G. E. M. Maguire and K. R. A. Sandanayake, *Chem. Soc. Rev.*, 1992, **21**, 187–195.
7. K. J. Naito, *Mater. Chem.*, 1998, **8**, 1379–1384.
8. I. Willner and B. J. Willner, *Mater. Chem.*, 1998, **8**, 2543–2556.
9. A. S. Lubbe, T. van Leeuwen, S. J. Wezenberg and B. L. Feringa, *Tetrahedron*, 2017, **73**, 4837–4848.
10. M. B. Avinash and T. Govindaraju, *Acc. Chem. Res.*, 2018, **51**, 414–426.
11. K. M. Roth, N. Dontha, R. B. Dabke, D. T. Gryko, C. Clausen, J. S. Lindsey, D. F. Bocian and W. G. Kuhr, *J. Vac. Sci. Technol. B*, 2000, **18**, 2359–2364.
12. D. T. Gryko, C. Clausen, K. M. Roth, N. Dontha, D. F. Bocian, W. G. Kuhr and J. S. Lindsey, *J. Org. Chem.*, 2000, **65**, 7345–7355.
13. D. T. Gryko, F. Zhao, A. A. Yasseri, K. M. Roth, D. F. Bocian, W. G. Kuhr and J. S. Lindsey, *J. Org. Chem.*, 2000, **65**, 7356–7362.
14. N. F. Borelli, J. B. Chodak and G. B. Hares, *J. Appl. Phys.*, 1979, **50**, 5978–5987.
15. D. D. Awschalom and J. M. Kikkawa, *Phys. Today*, 1999, **52**, 33–38.
16. H. Ohno, D. Chiba, F. Matsukura, T. Omiya, E. Abe, T. Dietl, Y. Ohno and K. Ohtani, *Nature*, 2000, **408**, 944–946.
17. R. L. Edelstein, C. R. Tamanaha, P. E. Sheehan, M. M. Miller, D. R. Baselt, L. J. Whitman and R. J. Colton, *Biosens. Bioelectron.*, 2000, **14**, 805–813.
18. D. Ruiz-Molina, G. Christou and D. N. Hendrickson, *Mol. Cryst. Liq. Cryst.*, 2000, **343**, 17–27.
19. R. Sessoli, D. Gatteschi, A. Caneschi and M. A. Novak, *Nature*, 1993, **365**, 141–143.
20. J. R. Friedman, M. P. Sarachick, J. Tejada and R. Ziolo, *Phys. Rev. Lett.*, 1996, **76**, 3830–3833.
21. J. M. Hernandez, X. X. Zhang, F. Luis, J. Bartolom, J. Tejada and R. Ziolo, *Europhys. Lett.*, 1996, **35**, 301–306.
22. D. Gatteschi and R. Sessoli, *Angew. Chem. Int. Ed.*, 2003, **42**, 268–297.
23. M. Clemente-León, H. Soyer, E. Coronado, C. Mingotaud, C. J. Gómez-García and P. Delhaes, *Angew. Chem. Int. Ed.*, 1998, **37**, 2842–2845.
24. G. C. Condorelli, A. Motta, I. L. Fragala, F. Giannazzo, V. Rainieri, A. Caneschi and D. Gatteschi, *Angew. Chem. Int. Ed.*, 2004, **43**, 4081–4084.
25. D. Ruiz-Molina, M. Mas-Torrent, J. Gómez, A. I. Balana, N. Domingo, J. Tejada, M. T. Martínez, C. Rovira and J. Veciana, *Adv. Mater.*, 2003, **15**, 42–45.
26. D. Ruiz-Molina, P. Gerbier, E. Rumberger, D. B. Amabilino, I. A. Guzei, K. Folting, J. C. Huffman, A. Rheingold, G. Christou, J. Veciana and D. N. Hendrickson, *J. Mater. Chem.*, 2002, **12**, 1152–1161.
27. R. Ballardini, P. Ceroni, A. Credi, M. T. Gandolfi, M. Maestri, M. Semararo, M. Venturi and V. Balzani, *Adv. Funct. Mater.*, 2007, **17**, 740–750.
28. D. Margulies, G. Melman and A. Shanzer, *Nat. Mater.*, 2005, **4**, 768–771.
29. D. Margulies, G. Melman and A. Shanzer, *J. Am. Chem. Soc.*, 2006, **128**, 4865–4871.
30. A. P. de Silva, M. R. James, B. O. F. Mckinney, D. A. Pears and S. M. Weir, *Nat. Mater.*, 2006, **5**, 787–789.
31. D. C. Magri, G. J. Brown, G. D. McClean and A. P. de Silva, *J. Am. Chem. Soc.*, 2006, **128**, 4950–4951.
32. S. Kawata and Y. Kawata, *Chem. Rev.*, 2000, **100**, 1777–1788.
33. A. Y. Bobrovsky, N. I. Boiko, V. P. Shibaev and J. Springer, *Adv. Mater.*, 2000, **12**, 1180–1183.
34. T. Asahi, M. Suzuki and H. Masuhara, *J. Phys. Chem. A*, 2002, **106**, 2335–2340.
35. A. K. Chibisov, V. S. Marevtsev and H. Görner, *J. Photochem. Photo-biol. A*, 2003, **159**, 233–239.
36. C.-C. Ko, L.-X. Wu, K. M.-C. Wong, N. Y. Zhu and V. W.-W. Yam, *Chem. Eur. J.*, 2004, **10**, 766–776.
37. A. Romani, G. Chidichimo, P. Formoso, S. Manfredi, G. Favaro and U. Mazzucato, *J. Phys. Chem. B*, 2002, **106**, 9490–9495.
38. V. W.-W. Yam, C.-C. Ko, L.-X. Wu, K. M.-C. Wong and K.-K. Cheung, *Organometallics* 2000, **19**, 1820–1822.
39. R. Nakao, F. Noda, T. Horii and Y. Abe, *Polym. Adv. Technol.*, 2002, **13**, 81–86.
40. S. Harrell, T. Seidel and B. Fay, *Microelectron. Eng.*, 1996, **30**, 11–15.
41. D. T. Gryko, C. Clausen and J. S. Lindsey, *J. Org. Chem.*, 1999, **64**, 8635–8647.
42. G.-W. Cha, C. Yo, N.-J. Kim, K.-Y. Kim, C. H. Lee, K.-N. Lim, K. Lee, J.-Y. Jeon, T. S. Jung, H. Jeong, T.-Y. Chung, K. Kim and S. I. Cho, *IEEE J. Solid-State Circuits*, 1999, **34**, 1589–1599.
43. R. H. Stulen and D. W. Sweeney, *IEEE J. Quantum Electron.*, 1999, **35**, 694–699.
44. C. P. Collier, E. W. Wong, M. Belohradsky, F. M. Raymo, J. F. Stoddart, P. J. Kuekes, R. S. Williams and J. R. Heath, *Science*, 1999, **285**, 391–394.
45. J. Chen, M. A. Reed, A. M. Rawlett and J. M. Tour, *Science*, 1999, **286**, 1550–1552.
46. C. S. Lent, *Science*, 2000, **288**, 1597–1599.
47. J. M. Tour, L. Jones II, D. L. Pearson, J. J. S. Lamba, T. P. Burgin, G. M. Whitesides, D. L. Allara, A. N. Parikh and S. Atre, *J. Am. Chem. Soc.*, 1995, **117**, 9529–9534.
48. K. Kastner, A. J. Kibler, E. Karjalainen, J. A. Fernandes, V. Sans and G. N. Newton, *J. Mater. Chem. A*, 2017, **5**, 11577–11581.
49. F. Hide, M. A. Díaz-García, B. J. Schwartz, M. R. Andersson, Q. Pei and A. J. Heeger, *Science*, 1996, **273**, 1833–1836.
50. X.-H. Zhu, J. Peng, Y. Cao and J. Roncali, *Chem. Soc. Rev.*, 2011, **40**, 3509–3524.
51. M. Santra, H. Moon, M.-H. Park, T.-W. Lee, Y. K. Kim and K. H. Ahn, *Chem. Eur. J.*, 2012, **18**, 9886–9893.
52. F. Schieber, *Proceedings of the Human Factors and Ergonomics Society Annual Meeting*, 2001, **45**, 1324–1327.
53. Z. Zhao, J. W. Y. Lam and B. Z. Tang, *J. Mater. Chem.*, 2012, **22**, 23726–23740.
54. C. Feldmann, T. Jüstel, C. R. Ronda and P. J. Schmidt, *Adv. Funct. Mater.*, 2003, **13**, 511–516.
55. I. Yoshimura, Y. Miyahara, N. Kasagi, H. Yamane, A. Ojida and I. Hamachi, *J. Am. Chem. Soc.*, 2004, **126**, 12204–12205.
56. M. Ikeda, K. Fukuda, T. Tanida, T. Yoshii and I. Hamachi, *Chem. Commun.*, 2012, **48**, 2716–2718.
57. H. Wang, X. Ji, Y. Li, Z. Li, G. Tang and F. Huang, *J. Mater. Chem. B*, 2018, **6**, 2728–2733.
58. H. Wang, X. Ji, Z. Li and F. Huang, *Adv. Mater.*, 2017, **29**, 1606117.
59. X. Ji, B. Shi, H. Wang, D. Xia, K. Jie, Z. L. Wu and F. Huang, *Adv. Mater.*, 2015, **27**, 8062–8066.
60. R. Chen and D. J. Lockwood, *J. Electrochem. Soc.*, 2002, **149**, S69–S78.
61. M. Born and T. Jüstel, *Phys. J.*, 2003, **2**, 43–49.
62. H. O. Jungk and C. Feldmann, *J. Mater. Res.*, 2000, **15**, 2244–2248.

63. J. P. Boeuf, *J. Phys. D: Appl. Phys.*, 2003, **36**, R53–R79.
64. H. A. Höppe, H. Lutz, P. Morys, W. Schnick and A. Seilmeier, *J. Phys. Chem. Solids*, 2000, **61**, 2001–2006.
65. Y. Izumi and Y. Yamane, *MRS Bull.*, 2002, 889.
66. X. Zhang, Z. Chi, B. Xu, L. Jiang, X. Zhou, Y. Zhang, S. Liu and J. Xu, *Chem. Commun.*, 2012, **48**, 10895–10897.
67. H. Y. Li, Z. G. Chi, B. J. Xu, X. Q. Zhang, Z. Y. Yang, X. F. Li, S. W. Liu, Y. Zhang and J. R. Xu, *J. Mater. Chem.*, 2010, **20**, 6103–6110.
68. Z. Y. Yang, Z. G. Chi, B. J. Xu, H. Y. Li, X. Q. Zhang, X. F. Li, S. W. Liu, Y. Zhang and J. R. Xu, *J. Mater. Chem.*, 2010, **20**, 7352–7359.
69. S. J. Yoon, J. W. Chung, J. Gierschner, K. S. Kim, M. G. Choi, D. Kim and S. Y. Park, *J. Am. Chem. Soc.*, 2010, **132**, 13675–13683.
70. X. L. Luo, J. N. Li, C. H. Li, L. P. Heng, Y. Q. Dong, Z. P. Liu, Z. S. Bo and B. Z. Tang, *Adv. Mater.*, 2011, **23**, 3261–3265.
71. C. D. Dou, L. Han, S. S. Zhao, H. Y. Zhang and Y. Wang, *J. Phys. Chem. Lett.*, 2011, **2**, 666–670.
72. X. Q. Zhang, Z. G. Chi, B. J. Xu, C. J. Chen, X. Zhou, Y. Zhang, S. W. Liu and J. R. Xu, *J. Mater. Chem.*, 2012, **22**, 18505–18513.
73. C. Huang, B. Lucas, C. Vervaet, K. Braeckmans, S. Van Calenbergh, I. Karalic, M. Vandewoestyne, D. Deforce, J. Demeester and S. C. De Smedt, *Adv. Mater.*, 2010, **22**, 2657–2662.
74. M. J. Dejneka, A. Streltsov, S. Pal, A. G. Frutos, C. L. Powell, K. Yost, P. K. Yuen, U. Muller and J. Lahiri, *Proc. Natl. Acad. Sci. U. S. A.*, 2003, **100**, 389–393.
75. X. Hou, C. Ke, C. J. Bruns, P. R. McGoniga, R. B. Pettman and J. F. Stoddart, *Nat. Commun.*, 2015, **6**, 6884.
76. S. Han, H. J. Bae, J. Kim, S. Shin, S.-E. Choi, S. H. Lee, S. Kwon and W. Park, *Adv. Mater.*, 2012, **24**, 5924–5929.
77. L. Zhu, Y. Yin, C.-F. Wang and Su Chen, *J. Mater. Chem. C*, 2013, **1**, 4925–4932.
78. H. Wang, X. Ji, Z. Li, C. N. Zhu, X. Yang, T. Li, Z. L. Wu and F. Huang, *Mater. Chem. Front.*, 2017, 1, 167–171.
79. G. De Cremer, B. F. Sels, J.-i. Hotta, M. B. J. Roeffaers, E. Bartholomeeusen, E. Coutiño-Gonzalez, V. Valtchev, D. E. De Vos, T. Vosch and J. Hofkens, *Adv. Mater.*, 2010, **22**, 957–960.
80. C.-N. Zhu, T. Bai, H. Wang, W. Bai, J. Ling, J.-Z. Sun, F. Huang, Z.-L. Wu and Q. Zheng, *ACS Appl. Mater. Interfaces*, 2018, **10**, 39343–39352.
81. X. Ji, R. T. Wu, L. Long, X. S. Ke, C. Guo, Y. J. Ghang, V. M. Lynch, F. Huang and J. L. Sessler, *Adv. Mater.*, 2018, **30**, 1705480.
82. X. Ji, W. Chen, L. Long, F. Huang and J. L. Sessler, *Chem. Sci.*, 2018, **9**, 7746–7752.
83. C. Shi, Y. Zhu, G. Zhu, X. Shen and M. Ge, *J. Mater. Chem. C*, 2018, **6**, 9552–9560.
84. J. Sun, J. Wang, M. Chen, X. Pu, G. Wang, L. Li, G. Chen, Y. Cai, X. Gu and B. Z. Tang, *Chem. Mater.*, 2019, **31**, 5683−5690.
85. S. E. Brunker, K. B. Cederquist and C. D. Keating, *Nanomedicine*, 2007, **2**, 695−710.
86. R. Wilson, A. R. Cossins and D. G. Spiller, *Angew. Chem. Int. Ed.*, 2006, **45**, 6104−6117.
87. N. H. Finkel, X. Lou, C. Wang and L. He, *Anal. Chem.*, 2004, **76**, 353A−359A.
88. M. Sha, I. Walton, S. Norton, M. Taylor, M. Yamanaka, M. Natan, C. Xu, S. Drmanac, S. Huang, A. Borcherding, R. Drmanac and S. Penn, *Anal. Bioanal. Chem.*, 2006, **384**, 658−666.
89. B. He, S. J. Son and S. B. Lee, *Anal. Chem.*, 2007, **79**, 5257−5263.
90. B. He, S. J. Son and S. B. Lee, *Langmuir*, 2006, **22**, 8263−8265.
91. S. R. Nicewarner-Pena, R. G. Freeman, B. D. Reiss, L. He, D. J. Pena, I. D. Walton, R. Cromer, C. D. Keating and M. J. Natan, *Science*, 2001, **294**, 137−141.
92. B. D. Reiss, R. G. Freeman, I. D. Walton, S. M. Norton, P. C. Smith, W. G. Stonas, C. D. Keating and M. J. Natan, *J. Electroanal. Chem.*, 2002, **522**, 95−103.
93. L. Qin, M. J. Banholzer, J. E.Millstone and C. A. Mirkin, *Nano Lett.*, 2007, **7**, 3849−3853.
94. J. B.-H. Tok, F. Y. S. Chuang, M. C. Kao, K. A. Rose, S. S. Pannu, M. Y. Sha, G. Chakarova, S. G. Penn and G. M. Dougherty, *Angew. Chem. Int. Ed.*, 2006, **45**, 6900−6904.
95. I. D. Walton, S. M. Norton, A. Balasingham, L. He, D. F. Oviso, D. Gupta, P. A. Raju, M. J. Natan and R. G. Freeman, *Anal. Chem.*, 2002, **74**, 2240−2247.
96. R. L. Stoermer, K. B. Cederquist, S. K. McFarland, M. Y. Sha, S. G. Penn and C. D. Keating, *J. Am. Chem. Soc.*, 2006, **128**, 16892−16903.
97. J. A. Sioss and C. D. Keating, *Nano Lett.*, 2005, **5**, 1779−1783.
98. J. A. Sioss, R. L. Stoermer, M. Y. Sha and C. D. Keating, *Langmuir*, 2007, **23**, 11334−11341.
99. W. Burns, *Bull. World Health Organ.*, 2006, **84**, 689−690.
100. P. Aldhous, *Nature*, 2005, **434**, 132−134.
101. A. Ault, *Lancet*, 2003, **362**, 301.
102. R. Cockburn, P. N. Newton, E. K. Agyarko, D. Akunyili and N. J. White, *PLoS Med.*, 2005, **2**, 302−308.
103. M. Larkin, *Lancet Infect. Dis.*, 2006, **6**, 552.
104. P. N. Newton, M. D. Green, F. M. Fernandez, N. P. J. Day and N. J. White, *Lancet Infect. Dis.*, 2006, **6**, 602−613.
105. T. Parfitt, *Lancet*, 2006, **368**, 1481−1482.
106. P. M. Rudolf and I. B. G. Bernstein, *N. Engl. J. Med.*, 2004, **350**, 1384−1386.
107. C. Schubert, *Nat. Med.*, 2008, **14**, 700.
108. C. Sheridan, *Nat. Biotechnol.*, 2007, **25**, 707−709.
109. F. Fayazpour, B. Lucas, N. Huyghebaert, K. Braeckmans, S. Derveaux, B. G. Stubbe, J. P. Remon, J. Demeester, C. Vervaet and S. C. De Smedt, *Adv. Mater.*, 2007, **19**, 3854−3858.
110. K. Braeckmans, S. C. De Smedt, C. Roelant, M. Leblans, R. Pauwels and J. Demeester, *Nat. Mater.*, 2003, **2**, 169−173.
111. K. Braeckmans, S. C. De Smedt, M. Leblans, R. Pauwels and J. Demeester, *Nat. Rev. Drug Discov.*, 2002, **1**, 447−456.
112. K. L. Michael, L. C. Taylor, S. L. Schultz and D. R. Walt, *Anal. Chem.*, 1998, **70**, 1242–1248.
113. M. Han, X. Gao, J. Z. Su and S. Nie, *Nat. Biotechnol.*, 2001, **19**, 631–635.
114. S. R. Nicewarner-Peña, R. G. Freeman, B. D. Reiss, L. He, I. D. Walton, R. Cromer, C. D. Keating and M. J. Natan, *Science*, 2001, **294**, 137–141.
115. M. Trau and B. J. Battersby, *Adv. Mater.*, 2001, **13**, 975–979.
116. X. Michalet, F. Pinaud, T. D. Lacoste, M. Dahan, M. P. Bruchez, A. P. Alivisatos and S. Weiss, *Single Mol.*, 2001, **2**, 261–276.
117. I. D. Walton, S. M. Norton, A. Balasingham, L. He, D. F. Oviso, D. Gupta, P. A. Raju, M. J. Natan and R. G. Freeman, *Anal. Chem.*, 2002, **74**, 2240–2247.
118. L. Li, T. Ruzgas and A. K. Gaigalas, *Langmuir*, 1999, **15**, 6358–6363.
119. X. H. Zhu, J. B. Peng, Y. Caoa and J. Roncali, *Chem. Soc. Rev.*, 2011, **40**, 3509–3524.
120. M. Santra, H. Moon, M. Park, T. Lee, Y. K. Kim and K. H. Ahn, *Chem. Eur. J.*, 2012, **18**, 9886–9893.

121. H. Sasabe, N. Toyota, H. Nakanishi, T. Ishizaka, Y. J. Pu and J. Kido, *Adv. Mater.*, 2012, **24**, 3212–3217.
122. K. Kumar, H. Duan, R. S. Hegde, S. C. W. Koh, J. N. Wei and J. K. W. Yang, *Nat. Nanotechnol.*, 2012, **7**, 557–561.
123. Y. Lu, J. Zhao, R. Zhang, Y. Liu, D. Liu, E. M. Goldys, X. Yang, P. Xi, A. Sunna, J. Lu, Y. Shi, R. C. Leif, Y. Huo, J. Shen, J. A. Piper, J. P. Robinson and D. Jin, *Nat. Photonics*, 2014, **8**, 32–36.
124. F. Hide, M. A. -DiazGarcia, B. J. Schwartz, M. R. Anderson, Q. Pei and A. J. Heeger, *Science*, 1996, **273**, 1833–1836.
125. A. K. Deisingh, *Analyst*, 2005, **130**, 271–279.
126. B. Yoon, J. Lee, I. S. Park, S. Jeon, J. Lee and J. M. Kim, *J. Mater. Chem. C*, 2013, **1**, 2388–2403.
127. J. S. Pan, H. C. Huang, L. C. Jain and W. C. Fang, *Intelligent Multimedia Data Hiding*, 2007, vol. 2, pp. 461–464.
128. J. S. Tan, *Synth. J.*, 2008, 59–78.
129. H. C. Huang andW. C. Fang, *Simul. Model. Pract. Th.*, 2010, **18**, 436–445.
130. H. C. Huang, F. C. Chang and W. C. Fang, *IEEE Trans. Consum. Electron.*, 2011, **57**, 779–787.
131. S. N. Baker and G. A. Baker, *Angew. Chem., Int. Ed.*, 2010, **49**, 6726–6744.
132. F. Wang, Z. Xie, H. Zhang, C. Y. Liu and Y. G. Zhang, *Adv. Funct. Mater.*, 2011, **21**, 1027–1031.
133. H. T. Li, Z. H. Kang, Y. Liu and S. T. Lee, *J. Mater. Chem.*, 2012, **22**, 24230–24253.
134. J. H. Shen, Y. H. Zhu, X. L. Yang and C. Z. Li, *Chem. Commun.*, 2012, **48**, 3686–3699.
135. S. C. Ray, A. Saha, N. R. Jana and R. Sarkar, *J. Phys. Chem. C*, 2009, **113**, 18546–18551.
136. R. L. Liu, D. Q. Wu, S. H. Liu, K. Koynov, W. Knoll and Q. Li, *Angew. Chem., Int. Ed.*, 2009, **48**, 4598–4601.
137. L. N. Thibos, A. Bradley, D. L. Still, X. Zhang and P. A. Howarth, *Vision Res.*, 1990, **30**, 33–49.
138. P. Kruger, S. Mathews, K. Aggarwala and N. Sanchez, *Vision Res.*, 1993, **33**, 1397–1411.
139. D. H. Marimont and B. A. Wandell, *J. Opt. Soc. Am. A*, 1994, **11**, 3113–3122.
140. B. J. Battersby, D. Bryant, W. Meutermans, D. Matthews and M. L. Smythe, M. Trau, *J. Am. Chem. Soc.*, 2000, **122**, 2138–2139.
141. B. J. Battersby, G. A. Lawrie and M. Trau, *Drug Discovery Today*, 2001, **6**, S19–S26.
142. B. J. Egner, S. Rana, H. Smith, N. Bouloc, J. G. Frey, W. S. Brocklesby and M. Bradley, *Chem. Commun.*, 1997, 735–736.
143. M. Trau and B. J. Battersby, *Adv. Mater.*, 2001, **13**, 975–979.
144. R. F. Harris, A. J. Nation, G. T. Copeland and S. J. Miller, *J. Am. Chem. Soc.*, 2000, **122**, 11270–11271.
145. J. T. Suri, D. B. Cordes, F. E. Cappuccio, R. A. Wessling and B. Singaram, *Angew. Chem., Int. Ed.*, 2003, **42**, 5857–5859.
146. P. Bairi, B. Roy and A. K. Nandi, *Chem. Commun.*, 2012, **48**, 10850–10852.
147. D. H. Park, C. J. Han, Y. G. Shul and J. H. Choy, *Sci. Rep.*, 2014, **4**, 4879.
148. S. Erevelles, N. Fukawa and L. Swayne, *J. Bus. Res.*, 2016, **69**, 897–904.
149. M. Li, X. Zheng and G. Zhuang, *J. Bus. Res.*, 2017, **78**, 268–276.
150. K. P. McDonald, B. Qiao, E. B. Twum, S. Lee, P. J. Gamache, C. H. Chen, Y. Yi and A. H. Flood, *Chem. Commun.*, 2014, **50**, 13285–13288.
151. Y. Li and A. H. Flood, *Angew. Chem., Int. Ed.*, 2008, **47**, 2649–2652.
152. 3 H. Aboubakr, H. Brisset, O. Siri and J. M. Raimundo, *Anal. Chem.*, 2013, **85**, 9968–9974.
153. R. Nishiyabu and P. Anzenbacher Jr, *Org. Lett.*, 2006, **8**, 359–362.
154. R. Nishiyabu and P. Anzenbacher Jr, *J. Am. Chem. Soc.*, 2005, **127**, 8270–8271.
155. H. Miyaji, W. Sato and J. L. Sessler, *Angew. Chem., Int. Ed.*, 2000, **39**, 1777–1780.
156. P. A. Gale and C. Caltagirone, *Chem. Soc. Rev.*, 2015, **44**, 4212–4227.
157. Y. Li, M. Gecevicius and J. Qiu, *Chem. Soc. Rev.*, 2016, **45**, 2090–2136.
158. H. Dong, S. R. Du, X. Y. Zheng, G. M. Lyu, L. D. Sun, L. D. Li, P. Z. Zhang, C. Zhang and C. H. Yan, *Chem. Rev.*, 2015, **115**, 10725–10815.
159. S. Gai, C. Li, P. Yang and J. Lin, *Chem. Rev.*, 2014, **114**, 2343–2389.
160. H. Wang, P. Wang, H. Xing, N. Li and X. F. Ji, *J. Polym. Sci., Part A: Polym. Chem.*, 2015, **53**, 2079–2084.
161. H. Wang, X. F. Ji, Z. T. Li and F. H. Huang, *Adv. Mater.*, 2017, **29**, 1606117.
162. H. Wang, X. F. Ji, Y. Li, Z. T. Li, G. P. Tang and F. H. Huang, *J. Mater. Chem. B*, 2018, **6**, 2728–2733.
163. H. Xing, H. Wang, X. Yan and X. Ji, *Dalton Trans.*, 2015, **44**, 11264–11268.
164. H. Wang, X. Ji, M. Ahmed, F. Huang and J. L. Sessler, *J. Mater. Chem. A*, 2019, **7**, 1394–1403.
165. B. J. Blaiszik, S. L. B. Kramer, S. C. Olugebefola, J. S. Moore, N. R. Sottos and S. R. White, *Annu. Rev. Mater. Res.*, 2010, **40**, 179–211.
166. Y. Cui, Y. Yue, G. Qian and B. Chen, *Chem. Rev.*, 2012, **112**, 1126–1162.
167. X.-P. He, X.-L. Hu, T. D. James, J. Yoon and H. Tian, *Chem. Soc. Rev.*, 2017, **46**, 6687–6696.
168. J.-L. Liu, Y.-C. Chen and M.-L. Tong, *Chem. Soc. Rev.*, 2018, **47**, 2431–2453.
169. H. Sun, S. Liu, W. Lin, K. Y. Zhang, W. Lv, X. Huang, F. Huo, H. Yang, G. Jenkins and Q. Zhao, *Nat. Commun.*, 2014, **5**, 3601.
170. P. Zijlstra, J. W. Chon and M. Gu, *Nature*, 2009, **459**, 410–413.
171. X. Liu, Y. Wang, X. Li, Z. Yi, R. Deng, L. Liang, X. Xie, D. T. Loong, S. Song and D. Fan, *Nat. Commun.*, 2017, **8**, 899.
172. Z. Li, H. Chen, B. Li, Y. Xie, X. Gong, X. Liu, H. Li and Y. Zhao, *Adv. Sci.*, 2019, 1901529.

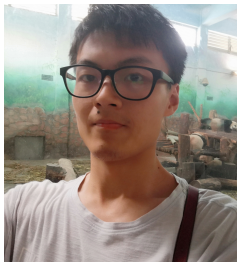

Hu Wang

Hu Wang was born in Anhui, China in 1990. He received his Bachelor of Science degree in Applied Chemistry from Xidian University, China. In June 2019, He completed his Ph.D. at Zhejiang University under the direction of Prof. Feihe Huang. From November 2016 to May 2017, he visited the group of Prof. Rafal Klajn at the Weizmann Institute of Science. As of September 2019, he has been working a Postdoctoral

Fellow jointly advised by Prof. Jonathan L. Sessler and Prof. Zachery Page at The University of Texas at Austin. His current studies are focused on functional materials constructed by non-covalent interactions and traditional polymer methods.

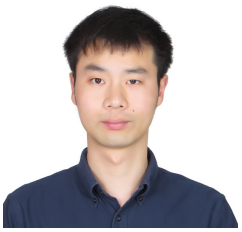

Xiaofan Ji

Xiaofan Ji completed his Ph.D. in June 2015 from Zhejiang University under the direction of Prof. Feihe Huang. From 2013 to 2014, he visited the group of Prof. Steven C. Zimmerman at the University of Illinois at Urbana-Champaign. After postdoctoral stays in the University of Tokyo (2015-2016, Prof. Takuzo Aida group), the University of Texas at Austin (2016-2018, Prof. Jonathan L. Sessler group), and the Hong Kong University of Science and Technology (2018-2019, Prof. Ben Zhong Tang group), he accepted a position as a full Professor of School of Chemistry and Chemical Engineering at Huazhong University of Science and Technology starting from December 2019. His current research interests involve fluorescent supramolecular polymeric materials.

Zachariah A Page

Prof. Zachery ("Zak") Page obtained his B.S. in Chemistry from Juniata College under the guidance of Prof. I. David Reingold. He spent three months abroad at the University of Cambridge, UK, working on the synthesis of novel conjugated polyelectrolytes under the aegis of Prof. Wilhelm Huck. After graduating from Juniata, Zak carried out his Ph.D. studies in the laboratories of Prof. Todd Emrick at the University of Massachusetts, Amherst. In 2015, he began his postdoctoral research with Prof. Craig J. Hawker at the University of California Santa Barbara. Zak assumed his current position of Assistant Professor in the Chemistry Department at The University of Texas at Austin in July 2018. His research interests are in the broad fields of macromolecular synthesis and materials science.

Jonathan L. Sessler

Jonathan L. Sessler received a BSc degree in Chemistry in 1977 from the University of California, Berkeley. He obtained his PhD from Stanford University in 1982. After postdoctoral stays in Strasbourg and Kyoto, he accepted a position as an Assistant Professor of Chemistry at the University of Texas at Austin, where he is currently the Doherty-Welch Chair. He was also a WCU Professor at Yonsei University and in 2015 accepted a laboratory directorate at Shanghai University. Professor Sessler is currently working on supramolecular chemistry, drug discovery, soft materials, and expanded porphyrin chemistry. He has published over 760 papers and his current h-index is 104.